

Masked Autoencoders in 3D Point Cloud Representation Learning

Jincen Jiang, Xuequan Lu, *Senior Member, IEEE*, Lizhi Zhao, Richard Dazaley, and Meili Wang, *Member, IEEE*

Abstract—Transformer-based Self-supervised Representation Learning methods learn generic features from unlabeled datasets for providing useful network initialization parameters for downstream tasks. Recently, methods based upon masking Autoencoders have been explored in the fields. The input can be intuitively masked due to regular content, like sequence words and 2D pixels. However, the extension to 3D point cloud is challenging due to irregularity. In this paper, we propose masked Autoencoders in 3D point cloud representation learning (abbreviated as MAE3D), a novel autoencoding paradigm for self-supervised learning. We first split the input point cloud into patches and mask a portion of them, then use our Patch Embedding Module to extract the features of unmasked patches. Secondly, we employ patch-wise MAE3D Transformers to learn both local features of point cloud patches and high-level contextual relationships between patches, then complete the latent representations of masked patches. We use our Point Cloud Reconstruction Module with multi-task loss to complete the incomplete point cloud as a result. We conduct self-supervised pre-training on ShapeNet55 with the point cloud completion pre-text task and fine-tune the pre-trained model on ModelNet40 and ScanObjectNN (PB_T50_RS, the hardest variant). Comprehensive experiments demonstrate that the local features extracted by our MAE3D from point cloud patches are beneficial for downstream classification tasks, soundly outperforming state-of-the-art methods (93.4% and 86.2% classification accuracy, respectively). Our source codes are available at: <https://github.com/Jinc98/MAE3D>.

Index Terms—Self-supervised learning, Point cloud, Completion

I. INTRODUCTION

Point cloud is a format of 3D data representation, which preserves the geometric information of 3D space, and is widely applied in autonomous driving, virtual reality, remote sensing and many other areas. In recent years, deep learning research on point clouds has developed rapidly, with promising results on tasks such as 3D point cloud shape classification and segmentation [1]–[8]. However, most existing methods require large labeled 3D point cloud datasets for supervised learning, which are expensive and time-consuming, driving the development of research on unsupervised point cloud learning.

Self-supervised learning is a type of unsupervised learning, i.e., training a neural network with supervisory signals generated by the data itself [9]. As a pioneer of Transformer-based self-supervised pre-training methods, BERT [10] has

made remarkable achievements in the field of natural language processing (NLP) by proposing the simple and effective masked language modeling pre-text task, which first randomly masks a portion of tokens within a text and then recovers the masked tokens by the Transformer. Inspired by BERT, several self-supervised vision representation models have been designed. BEiT [11] introduces a masked image modeling task to pre-train the visual Transformer. They tokenize the original input image as discrete visual tokens, and input image patches (some patches are randomly masked) into the Transformer backbone to recover the tokens of masked patches. He *et al.* [12] presents the masked Autoencoders (MAE) method, which randomly masks the patches of the image and inputs the visible patches subset to the encoder to obtain the latent representations, which are then concatenated with the mask tokens and input to the decoder to reconstruct the missing pixels of the original input image.

However, due to the gap between 3D point cloud data and image/text data, BERT-style self-supervised pre-training models cannot be directly applied to point clouds. Unlike text data with well-defined language vocabulary, point clouds do not have the concept of word in the NLP domain for the Transformer’s input unit. In addition, unlike regular pixels, point clouds have irregular point distributions, and it is more challenging to extract contextual relationships between local patches than image patches with grid structure. Point-BERT [13] makes an attempt to apply the BERT-style model to self-supervised 3D representation learning by devising the Masked Point Modeling (MPM) task to pre-train the Transformer. They propose a point cloud Tokenizer to generate discrete point tokens (i.e., discrete integer number) and divide the point cloud into local patches, which are then randomly masked. The goal of the MPM task is to train the Transformer to recover the initial discrete point tokens of the masked local patches. However, since Point-BERT requires an additional pre-trained Tokenizer, their approach is relatively complicated and time-consuming. In addition, their model cannot learn high-level features directly without the help of MoCo [14] to enhance the feature extraction ability of Transformers. More recently, some point cloud learning methods also take account of MAE. Point-MAE [15] uses Transformer based masked Autoencoder to reconstruct the point cloud. They only use a fully connected layer as a prediction head to generate masked points and compute the reconstruction loss for every mask patch individually. MaskPoint [16] trains a discriminator after the Transformer decoder to distinguish whether mask points are real or fake points, and underestimates the reconstruction of the entire point cloud. Point-M2AE [17] conducts a reconstruction task

J. Jiang, L. Zhao and M. Wang are with the College of Information Engineering, Northwest A&F University, China (e-mail: jinec@nwfufu.edu.cn; zhaolizhi@nwfufu.edu.cn; wml@nwsuaf.edu.cn)

X. Lu is with the Department of Computer Science and IT, La Trobe University, Australia (e-mail: b.lu@latrobe.edu.au)

R. Dazaley is with the School of Information Technology, Deakin University, Australia (e-mail: richard.dazeley@deakin.edu.au)

Manuscript received August 8th, 2022; accepted September 10th, 2023.

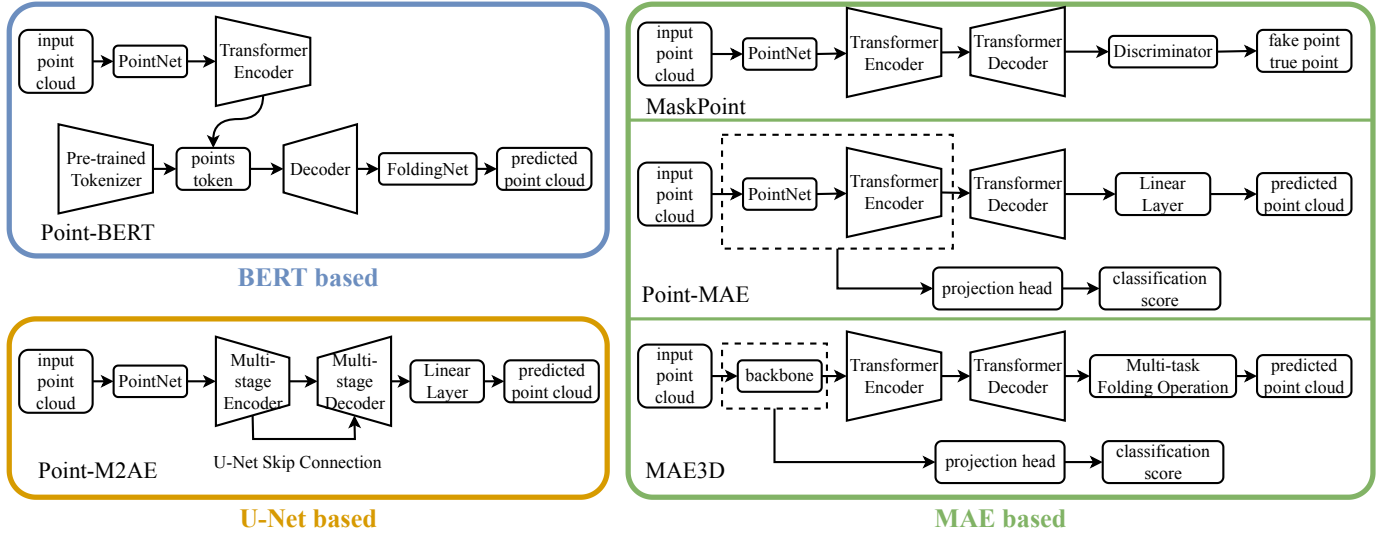


Fig. 1. Comparison of some recent works based on MPM pre-text task. We propose a masked Autoencoder based method (MAE3D) which is more general and lightweight and focuses more on point cloud reconstruction.

with multi-stage masking, but they utilize a hierarchical U-Net instead of Transformer blocks to learn latent features at different levels. Note that, all the above methods use a regular network, i.e., PointNet [1], as patch embedding to extract the features of each patch. In addition, they use a simple linear layer to predict each local patch’s coordinates discretely, ignoring the geometric relationship between each patch and the overall surface continuity of the point cloud during reconstruction.

Motivated by the above analysis, we propose 3D masked Autoencoders (MAE3D), a simple yet effective autoencoding paradigm for 3D point cloud self-supervised representation learning, to conduct the MPM pre-text task. We attempt to develop a general and lightweight framework making different point-based networks suit our paradigm. In this case, as shown in Figure 1, we load only the backbone network in the downstream task without introducing additional parameters, i.e., the heavy transformer blocks. Further, we propose a multi-task folding operation, focusing more on the point cloud reconstruction task, which enables the network to learn both the patches relationship and the entire point cloud geometry structure. Specifically, our MAE3D first splits the input point cloud into patches by k-nearest neighborhood (KNN) algorithm, and mask a portion of these patches, which are subsequently completed. Our MAE3D consists of three main components: Patch Embedding Module, MAE3D Transformers and Point Cloud Reconstruction Module. We devise the Patch Embedding Module with a patch feature extractor to extract latent representations of visible patches, which are concatenated with positional embedding and fed into MAE3D Transformers to complete the latent representations of masked patches. We then generate the entire point cloud global features by pooling the patch-wise latent representations and feed into our Point Cloud Reconstruction Module using our multi-task reconstruction loss to complete the incomplete point cloud. After the pre-training phase, we load only the pre-trained

patch feature extractor of Patch Embedding Module as our pre-trained model and evaluate it with 3D object classification as the downstream task.

The main contributions of this paper are:

- 1) We propose MAE3D, a novel and effective Transformer-based self-supervised representation learning method with masked Autoencoder for 3D point cloud data, learning both local features of point cloud patches and the high-level contextual relationships between patches.
- 2) Our MAE3D is lightweight and suitable for various point-based backbone networks. Only the pre-trained patch feature extractor is used for downstream tasks, without any additional parameters.
- 3) We design a multi-task loss for reconstruction, enabling the network to learn both the geometry structure of local patches and the overall surface continuity of the entire point cloud.
- 4) We conduct experiments and results show that our method pre-training on ShapeNet55 and fine-tuning on ModelNet40/ScanObjectNN soundly outperforms state-of-the-art techniques on the classification task, achieving 93.4% and 86.2% classification accuracy, respectively.

II. RELATED WORK

A. Supervised point cloud learning

As a pioneer of point-based learning methods that directly consume raw point cloud representation without voxelization or projection, PointNet [1] leverages the symmetry of max-pooling to learn the permutation-invariance features of point clouds. PointNet++ [4] devises a hierarchical architecture that recursively partitions the point cloud to extract local features more effectively, achieving better results than PointNet. DGCNN [2] is a graph-based method that creates a dynamic graph in the feature space and designs EdgeConv to learn the edge features of the graph in each layer. Point Cloud Transformer (PCT) [5] applies the traditional Transformer

[18] to point cloud learning by constructing an order-invariant attention mechanism based on the Transformer. Qiu *et al.* [19] presented a network that takes into account both low-level geometric information of 3D space points directly and high-level local geometric context of feature space implicitly.

B. Unsupervised point cloud Learning

Yang *et al.* propose FoldingNet [3], an end-to-end auto-encoder network for unsupervised learning of point clouds. They propose a novel folding-based decoder to transform the 2D grid onto a 3D surface represented by point cloud, achieving low reconstruction errors. MAP-VAE [20] learns global and local features of point clouds by combining global and local self-supervision. LatentGAN [21] proposes a deep Autoencoder architecture to train a minimal GAN in the Autoencoder's latent space to learn point cloud representations. Jiang *et al.* [22] propose an unsupervised contrast learning method for point clouds. They extract the feature representations of the original point cloud and its transformed version through a shared encoder.

C. Pre-training Transformers

Masked language model (MLM) proposed by BERT [10] discards a portion of the input sequence and trains the model with supervised signals generated from the input sequence itself to recover the missing content. BERT has greatly contributed to the research of pre-training Transformers. Following BERT, BEiT [11] proposes the masked image modeling (MIM) task for self-supervised visual representation learning. BEiT first takes the discrete VAE [23] as the image tokenizer, which tokenizes the image into discrete visual tokens. In the pre-training phase, BEiT randomly masks a portion of image patches, and feeds these corrupted patches into Transformer to learn to recover the visual tokens of the original image. More recently, MAE [12] has proposed a more effective asymmetric encoder-decoder architecture for MIM tasks, where the encoder operates on the visible patches to extract the latent representation by a linear projection with concatenated positional embeddings. A lightweight decoder reconstructs the original image from the latent representation and mask tokens.

Yu *et al.* [13] propose a BERT-style point cloud self-supervised representation learning model, named Point-BERT, to pre-train Transformer model through MPM task. The differences between Point-BERT and our MAE3D are significant: 1) they require additional pre-training of a DGCNN-based Variation AutoEncoder (dVAE) and rely heavily on contrastive learning, while we directly use the patch embedding module to obtain the latent features of each patch and consider them as tokens, thus avoiding extra computational overhead. 2) Their mask tokens are fed into the Transformer encoder, leading to early leakage of the location information, which is harmful to the latent feature of the network learning. By contrast, we replace the mask patches with a learnable mask token and take it as input to the Transformer decoder to force the encoder to focus on learning features from visible patches. 3) They use a tokenizer to generate discrete integer point tokens as a self-supervised signal. We directly complete the

latent representation of masked patches to reconstruct the point cloud, focusing more on the reconstruction task instead of predicting discrete point tokens.

We also elaborate the differences between some recent MAE-based works and our method: 1) Point-MAE [15] uses a simple linear layer as a prediction head to reconstruct the point cloud. By contrast, we use the folding operation, which can guarantee the continuity of the surface with better results. In addition, they only compute the loss for every mask patch, while our proposed multi-task loss first determines the location of each patch, then reconstructs their details by folding operation, and finally consolidates them to form a complete point cloud, ensuring the detail and continuity of the point cloud. 2) MaskPoint [16] trains the decoder to distinguish between the real and fake points instead of reconstructing the point cloud directly from latent features. 3) Point-M2AE [17] is not a Transformer-based network, but a hierarchical U-Net, which only learns features at different levels with masking strategy. Additionally, their multi-scale masking strategy reduces the mask region significantly after back-projecting, thus providing more input points, whereas we mask directly on the original input point cloud.

III. METHOD

Our MAE3D contains three main components: Patch Embedding Module, MAE3D Transformers, and Point Cloud Reconstruction Module. We first pre-train our model with MPM pre-text task, then fine-tune the pre-trained model with 3D object classification as the downstream task to verify its effectiveness. Figure 2 shows the architecture of our work.

A. Patch Embedding Module

In this part, we demonstrate the Patch Embedding Module to map the geometric information of the point cloud into latent representations. 3D point clouds are characterized by random order and irregular structure, and the irregularity of the input point clouds is aggravated by masking parts of the point cloud in the MPM pre-text task, which makes it difficult to obtain the embedding features by a simple linear projection as MAE [12] and ViT [24] do for image patches. To complete our MPM pretraining task, we first split point clouds into patches, then randomly mask a portion of them and feed these unmasked patches subset into our patch feature extractor to obtain the patch embedding features.

Patch split. We treat the point cloud patch as the word of the BERT-style framework. Given a point cloud $P \in \mathbb{R}^{N \times 3}$ with N points, we first uniformly downsample it to a sampled point cloud $P_c = \{c_i\}_{i=1}^S \in \mathbb{R}^{S \times 3}$ with S points by farthest point sampling (FPS), where each point in P_c is used as the center point of a patch. For each point c in P_c , we use the KNN algorithm to find a subset of local neighborhood centered on c from P , and define all these subsets as point cloud patches $Q = \{P_i\}_{i=1}^S$. The FPS can generally distribute the center point of each patch evenly, which encourages these patches to cover all points of P without duplication, i.e., $Q \approx P$.

Masking. We mask a part of the point cloud patches ($Q_M = \{P_i\}_{i \in m}$, m is the sequence of the masked patch index) and

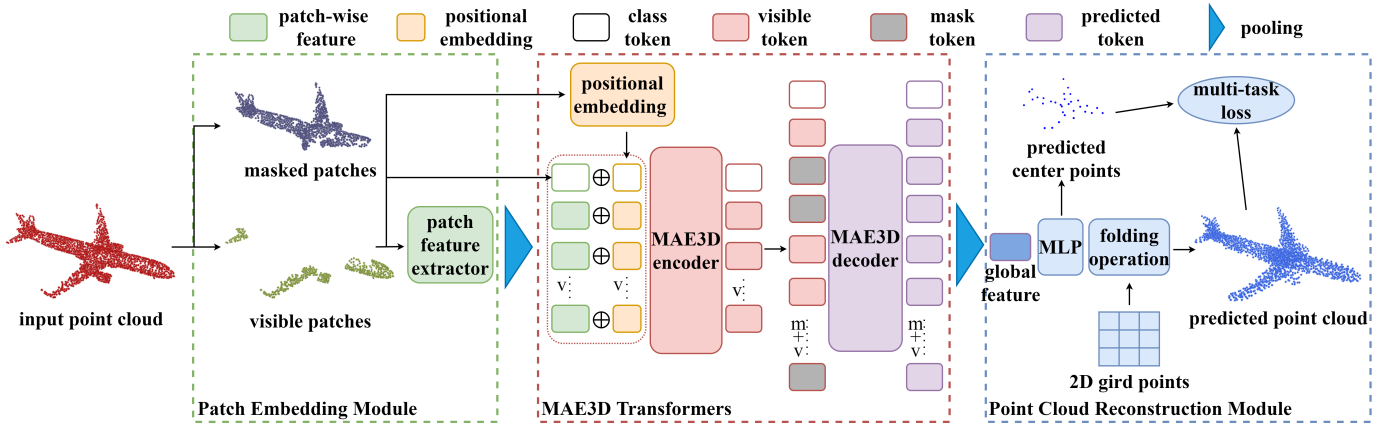


Fig. 2. Our MAE3D architecture. The input point cloud is split into patches and mask out a large portion of them. The remaining visible patches are fed to the patch feature extractor to obtain patch-wise features, adding positional embedding and class tokens, then passing them to MAE3D Transformers. The completed global features will be predicted by Transformers and used to reconstruct the point cloud. We develop a multi-task loss to measure both the predicted center points of patches and the reconstructed point cloud.

take these remaining unmasked patches ($Q_V = \{P_i\}_{i \in v}$, v is the sequence of visible patch index) as input. Specifically, we first randomly shuffle the list of patch indexes and remove that last part based on the masking ratio. The remaining patches are considered as visible patches which are then fed into the network. There are two masking strategies: random masking and block masking. For random masking, we randomly and uniformly select a subset of Q and remove it. For block masking, we first select a random point c_r in P_c , and calculate the K -nearest neighborhood of c_r from P_c , then we remove patches in Q corresponding to the point in that neighborhood. Experimental results of these two strategies can be seen in Section IV-C.

We completed our MPM pre-training task with a high masking ratio, i.e., 0.7, making the task more difficult and challenging, to better learn the latent representations from the unmasked visible patches Q_V . Meanwhile, a more sparse point cloud input would also make our network more efficient.

An image can be split into a sufficient number of patches, and each of them contains enough pixel information [12]. However, for point clouds, each patch has only a small number of points, e.g., 64 points, and the number of split patches is very limited, e.g., only 32 patches. Therefore, we choose the block masking strategy, which can preserve as much as possible the local spatial structure information of the remaining point cloud with a small number of points, which facilitates the network to obtain its latent representations.

Patch feature extractor. Point-based networks, such as PointNet [1] and DGCNN [2], usually include a pooling layer to output global features of a point cloud. The former part before the pooling layer of these networks, i.e., a series of multi-layer perceptions (MLPs), can be naturally treated as the feature extractor $\Psi(\psi | Q)$ to obtain the latent representations of the input visible patch $\{\psi_i\}_{i \in v} = \Psi(Q_V)$ in our MAE3D framework. In this case, we can simply use the former part of any point-based network as our feature extractor. In this work, we take the individual patch-wise subsets as input, with the feature extractor capturing the local features of each patch.

B. MAE3D Transformers

MAE3D is in charge of recovering the latent representations of the missing area of the point cloud and predicting the whole point cloud information (i.e., point cloud global feature) with the limited input. Following the BERT-style manner, in this work, we use the standard Transformer that contains a series of Self-Attention layers and FNN blocks. We use an asymmetric structure, where the encoder focuses on only part of the point cloud (i.e., the visible patch), and the decoder reconstructs the whole point cloud global feature by encoded patches and mask tokens.

Positional embedding. The positional embedding allows the operator in Self-Attention layers to well capture the contextual relationships of the input data. In image grids, the embedding of image patches is usually based on the sequence index using a trigonometric-based positional embedding method. However, in 3D data, the coordinates of each point naturally contain information about its position. Therefore, for each point cloud patch, we use its center point to represent the patch positional information with a trainable embedding layer. All patches' positional embedding can be defined as $\Phi(c_i) = \{\phi_i\}_{i=1}^S$. The embedding function Φ is an MLP.

MAE3D encoder. Our MAE3D encoder is formed by a series of Transformer blocks, and only applied to the visible patch Q_V . We concatenate the latent representations $\{\psi_i\}_{i \in v}$ obtained from each visible patch by the patch feature extractor and its positional embedding $\{\phi_i\}_{i \in v}$ together as the input embedding $\{x_i\}_{i \in v} = \{\text{concat}(\psi_i, \phi_i)\}_{i \in v}$. Inspired by ViT [24], we also put a class token Θ_0 in front of the input sequence, which is formed by a random parameter of trainable vector ψ_0 and a randomly initialized positional embedding ϕ_0 , i.e., $\Theta_0 = \text{concat}(\psi_0, \phi_0)$. The input to the MAE3D encoder can be denoted as $\chi = \{\Theta_0, x_i\}_{i \in v}$, which are then processed through a series of Transformer blocks. Similar to MAE [12], we discard the masked patches directly and do not use any mask tokens in the encoder part, which will save the computational time and memory effectively.

MAE3D decoder. For the missing area, we first define mask tokens $\{\tilde{\xi}_i\}_{i \in m}$ to represent the corresponding masked patch Q_M that need to be predicted, which consist of a set of randomly initialized learnable latent representations $\{\tilde{\psi}_i\}_{i \in m}$ and the positional embedding $\{\phi_i\}_{i \in m}$ of the missing patches. We provide the center point coordinates of each mask patch to compute the corresponding positional embedding, but the true locations of all points in each masked patch are not involved during the whole process. Similarly, we concatenate the initial latent representations and positional embedding to form the mask token as $\{\tilde{\xi}_i\}_{i \in m} = \{\text{concat}(\tilde{\psi}_i, \phi_i)\}_{i \in m}$.

Our MAE3D encoder will output the encoded visible patches, called visible tokens $\{\xi_i\}_{i \in v}$. Since the MAE3D encoder and decoder have different dimensions, we use a linear layer to match their dimensions. After that, we append a list of mask tokens at the end of visible tokens and unshuffle the entire token list (inverse of random shuffle) to align all tokens. The input to the decoder consists of all patches tokens (i.e., both visible tokens and mask tokens) and class token, which can be defined as $\Xi = \{\Theta_0, \xi_i, \xi_j\}_{i \in v, j \in m}$. The decoder has another series of Transformer blocks, and we simply use the standard Transformer following ViT [24] in image tasks. It is worth noting that during the whole process of our MAE3D Transformers, each point cloud patch will be viewed as an individual sample, i.e., MAE3D is a patch-wise approach. The output of the decoder will be a series of feature vectors representing each patch. We concatenate them in the point-wise dimension and then use a pooling layer to fuse the feature vectors into the global feature of the whole point cloud, which will be used for the pre-text task.

C. Point Cloud Reconstruction Module

The Point Cloud Reconstruction Module is responsible for generating the output point cloud from the global feature. Folding-based methods, like FoldingNet [3] and PCN [25], utilize the folding operation to achieve this task. Motivated by these methods, we develop a patch-based strategy for our MAE3D approach, which can effectively reconstruct the point cloud.

Patch center prediction. Similar to PCN [25], we also adopt a series of MLPs to generate a coarse point cloud \tilde{P}_c as the first step. The MLPs enable better prediction of a sparse set of points to represent the approximate shape of the point cloud. A key point in our method is that this coarse point cloud contains a very small number of points, i.e., 32 points, representing the center of each patch, which correspond to the P_c . Compared to previous works such as FoldingNet and PCN, which prioritize dense point cloud reconstruction but neglect structural information, our method introduces patch center prediction to improve the accuracy of the spatial location of each patch via the coarse point cloud output in the first stage, which leads to more faithful reconstructed results to the ground truth, depicting the more precise geometric shape of each patch and contextual relationships between patches.

Folding-based patch deformation. In this part, for the predicted center of each patch, we use 2D grid points (i.e., 8 rows \times 8 colons, totally have 64 points) to generate each

point in the patch with folding operation, and the number of each grid will exactly match the real patch. This folding operation takes the feature of the predicted center point and 2D grid as input and reconstructs a complete point cloud via deforming the grid. With our improved strategy, we can reduce the computation and storage by avoiding the redundant points generated by PCN [25], and the comparison between the predicted output \tilde{P} and ground truth P is much more sensible.

Reconstruction. Our MAE3D reconstructs a complete point cloud by predicting the features of each masked patch via inputting portion of the point cloud. With our Point Cloud Reconstruction Module, the predicted global feature of the point cloud can be reconstructed into a point cloud output. Our multi-task reconstruction loss function measures the Chamfer Distance (CD) between the reconstructed point cloud and the original one as well as the predicted center points of patches and the ground truth ones. Unlike MAE [12] that calculates loss only on masked patches, we will compute the loss on the entire point cloud. The Chamfer Distance can be defined as:

$$\text{CD}(S_1, S_2) = \frac{1}{|S_1|} \sum_{x \in S_1} \min_{y \in S_2} \|x - y\|_2^2 + \frac{1}{|S_2|} \sum_{y \in S_2} \min_{x \in S_1} \|y - x\|_2^2, \quad (1)$$

which calculates the average nearest point distance between the predicted point cloud S_1 and the ground truth point cloud S_2 .

Our multi-task loss function uses this metric twice to measure both predicted patch center \tilde{P}_c and predicted entire point cloud \tilde{P} , which can be formulated as:

$$L = \text{CD}(\tilde{P}_c, P_c) + \alpha \text{CD}(\tilde{P}, P), \quad (2)$$

where α is the hyper-parameter representing the weight of the latter term. This multi-task loss jointly uses the center point of each patch and the complete point cloud as self-supervised signal for point cloud completion. Our method first locates each center point position of each patch, then reconstructs their details through the folding operation, and processes the entire point cloud. Thus, the center point prediction enables the network to learn the geometry relationship between each patch effectively. By contrast, Point-MAE [15] only predicts each masked patch without considering either the position of the center point of each patch or the continuity of the entire point cloud.

D. Downstream Task

We use 3D object classification as our downstream task in this work to validate the performance of our MAE3D pre-text task pre-training. We take the former part of the backbone network (i.e., the patch feature extractor in Section III-A) as the pre-trained model which contains valuable parameters. In particular, the local feature and the spatial information of point cloud patches will be of great help for the downstream classification task.

We utilize two schemes to verify the capability of the pre-trained model. The first scheme is to use the pre-trained parameters to initialize the backbone and perform supervised training. The other one is to freeze the pre-trained model so

that they will not be trained in the downstream task, and only train a linear classifier to classify the learned representations of this pre-trained model (i.e., self-supervised learning). We will demonstrate the classification results for these two validation schemes and the shape part segmentation task in Section IV.

IV. EXPERIMENTAL RESULTS

A. Datasets

Completion pre-training. We use ShapeNet55 [26] as our pre-training dataset, which has 57,448 models with 55 categories, and all models will be used for the completion task to learn latent features. For each input point cloud, we divide them into 32 point patches which have 64 points for 2,048 points inputs. Then, we choose some patches to be masked with block or random mask sampling strategy. The rest of them, i.e., visible patches, will be used as input to the network.

Object classification. We utilize ModelNet40 [7] for 3D object classification. We follow the same data split protocols of previous methods, like PointNet [1] and DGCNN [2]. The dataset contains 9,840 models for training and 2,468 models for testing, which consists of 40 categories. We use 1,024 points with (x, y, z) normalized positions per model as the input, which is the same as previous works.

We also evaluate our method for the transfer learning on ScanObjectNN dataset [27], which contains 2,902 unique object instances from 15 categories. The objects are real-world point clouds based on the scanned indoor scene data. This dataset poses great challenges for the classification task, due to the involved background and incomplete data. We follow the official data split strategy, and conduct experiments on PB_T50_RS which is the most challenging dataset.

Shape part segmentation. We verify our method on shape part segmentation using ShapeNet Part dataset [28], which contains 16,881 shapes from 16 categories. Each shape has 2 to 6 parts, consisting of 50 specific part labels in total. We follow the official splits and point cloud sampling protocol in [26]. Only the point coordinates are used as the input.

B. Experimental Setting

We use Adam optimizer for all our experiments and implement our work with PyTorch. Unlike DGCNN [2] that uses multiple GPUs, we only use a single TITAN RTX GPU for training. For the pre-training completion task, we use a batch size of 32 for training. We use the dropouts of 0.5 and the random seed 1, which are the same as DGCNN. The learning rate is set to 0.0001 under the cosine learning scheduler with the 0.0001 weight decay. We train our model for 300 epochs and choose the last checkpoint as our pre-trained model. For downstream 3D object classification on ModelNet40 [7] and ScanObjectNN [27], we set the training batch size to 32 for all experiments. The other settings follow DGCNN. Our method achieves comparable results without any voting strategy during testing. For fair comparison, we use the results without voting by other papers.

TABLE I
COMPARISON RESULTS OF OUR METHOD AND SOTA TECHNIQUES ON THE COMPLETION TASK FOR PRE-TRAINING (CHAMFER DISTANCE) AND THE CLASSIFICATION TASK FOR FINE-TUNING (CLASSIFICATION ACCURACY). DGCNN IS USED AS BACKBONE IN OUR PATCH EMBEDDING MODULE.

Methods	# Points	Masking strategy	Masking ratio	CD ($\times 10^{-3}$)	Acc.
FoldingNet [3]	1k	block	0.7	6.858	90.4
PCN [25]	1k	block	0.7	4.394	90.7
Point-BERT [13]	1k	block	[0.25, 0.45]	-	93.2
Point-BERT [13]	1k	block	[0.55, 0.85]	-	92.6
MAE3D	1k	block	0.7	3.127	93.4

C. MAE3D Completion Pre-training

We experiment with the completion of 3D point clouds, which is the pre-text task for our method. Our MAE3D pre-training can be implemented simply and effectively. First, we remove a part of the point cloud by the block masking strategy and use the remaining point cloud as the input of the Patch Embedding Module. Then we predict the latent representation of missing parts by MAE3D Transformers, and finally, fuse the patch-wise features into the global feature to generate the point cloud output using the Point Cloud Reconstruction Module.

We visualize the results of our method in Figure 3. It can be found that the output point cloud can be reconstructed well by our method with only inputting a small part of points. We also compare our method with some previous methods, like FoldingNet [3] and PCN [25], under the same settings. Since we do not have the test set in the pre-trained reconstruction task and should use the augmentation during the training stage, we provide the complete output and ground truth corresponding to the input of different transformations for each sample. Our MAE3D can accurately predict the masked patches, producing the best reconstructed point clouds among the compared methods. This confirms that our MAE3D Transformers can obtain better local features of the point cloud patches and therefore our Point Cloud Reconstruction Module can further output more accurate point clouds.

We also calculate the Chamfer Distance of our MAE3D and some state-of-the-art (SOTA) methods, illustrated in Table I. To provide a fair comparison, we re-implement and then train two most relevant methods (FoldingNet [3] and PCN [25]) with the same masking strategy and masking ratio, i.e., the input are the same. It can be figured that our MAE3D can obtain the best results, which has the smallest error for the reconstructed output, and the pre-trained model also performs best in fine-tuning downstream task. In addition, we compared our MAE3D with Point-BERT [13], and we use their reported results directly. It is worth mentioning that they input more points, i.e., a smaller masking ratio, and we still outperform them by 0.2% on the downstream classification task.

D. 3D Object Classification

Pre-training evaluation. In this experiment, we select PointNet [1] and DGCNN [2] as the backbone. After our MAE3D pre-training, we initialize the former part of the backbone (i.e., the feature extractor with a pooling layer)

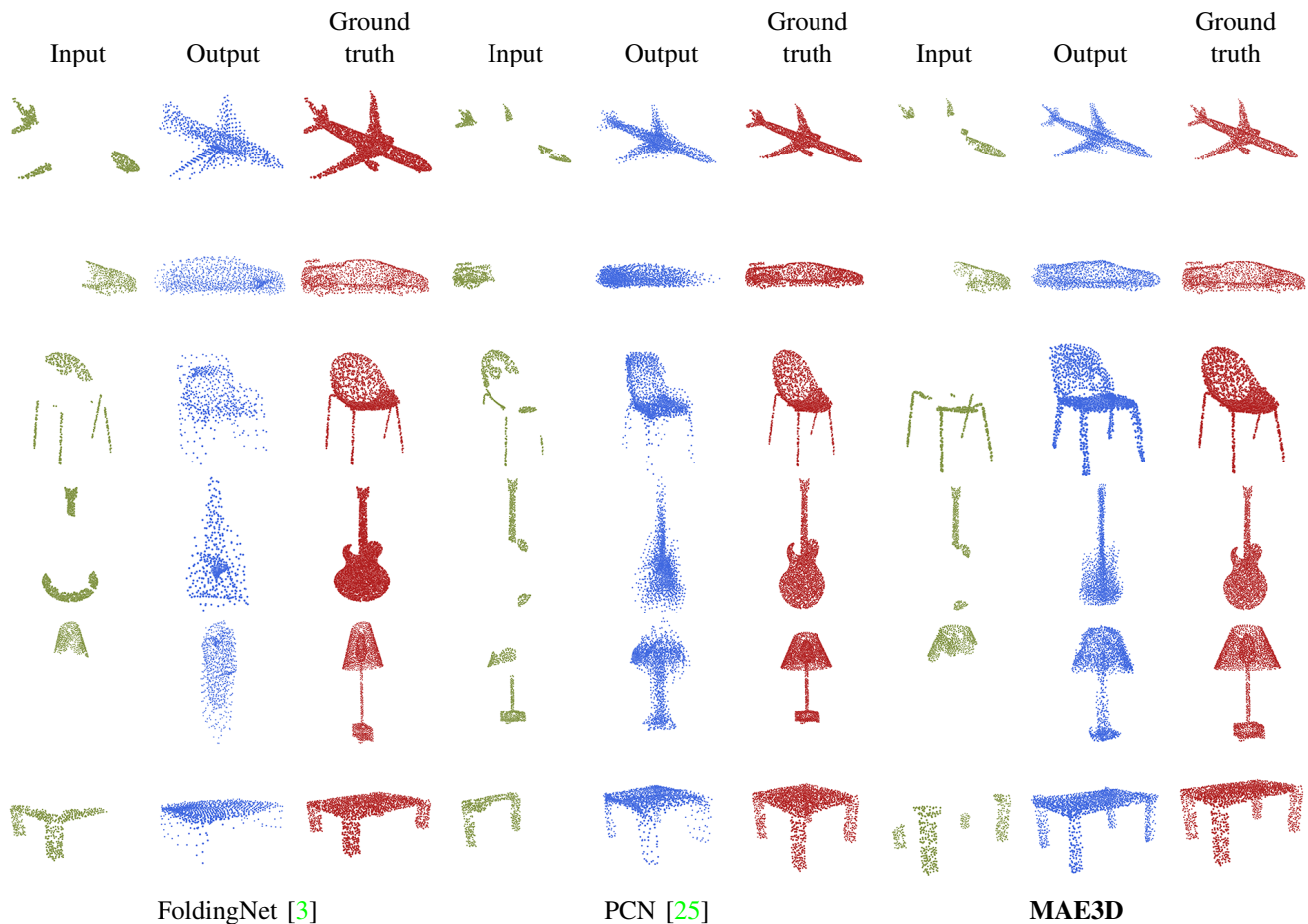


Fig. 3. Comparison of sample completion results between our MAE3D and other SOTA methods with 0.7 block masking ratio.

with the pre-trained model, which is used to obtain a global feature of the point cloud. The remaining classification branch (i.e., several MLPs) will be randomly initialized. We do not include the Transformer encoder in the downstream task network because it involves a series of blocks, which is a heavy structure, and including them affects the convergence of classification through experimental observation. The patch feature extractor merely is more lightweight and generalized to different point-based backbones.

As shown in Table II, the pre-training evaluation based on MAE3D sees a significant improvement over the original backbone network, with an increase of 1.4% on PointNet and 0.5% on DGCNN. It is worth noting that MAE3D achieves the best result of 93.4% using DGCNN as the backbone, which is comparable with any other SOTA method. In addition, we perform experiments on ModelNet10 and obtain the best results of 95.5% (in Table III), which exceeds all compared SOTA methods.

We also executed the classification experiment utilizing real-world data. This was conducted using all three variations found in ScanObjectNN: OBJ_ONLY, OBJ_BG, and PB_T50_RS. The results are presented in Table IV. From the results, it can be inferred that our pre-trained model garners an impressive result of 86.2% with fine-tuning on one of the most challenging variants PB_T50_RS. This performance surpasses both Point-MAE and PointMask by 1.0% and 1.6%,

TABLE II
CLASSIFICATION COMPARISON RESULTS OF OUR METHOD AND SUPERVISED METHODS ON MODELNET40. ALL RESULTS ARE WITHOUT THE VOTING STRATEGY.

Methods	Pre-trained	# Points	Acc.
PointNet++ [4]	-	1k	90.7
HAPGN [29]	-	1k	91.7
PointCNN [30]	-	1k	92.5
PointConv [6]	-	1k	92.5
RSCNN [31]	-	1k	92.9
PCT [5]	-	1k	93.2
SO-Net [32]	✓	2k	90.9
3Dpatch [33]	✓	1k	92.4
SSC (RSCNN) [34]	✓	1k	93.0
Point-BERT [13]	✓	1k	93.2
Point-MAE [15]	✓	1k	93.2
Point-M2AE [17]	✓	1k	93.4
PointNet [1]	-	1k	89.2
MAE3D (PointNet)	✓	1k	90.6 (+1.4)
DGCNN [2]	-	1k	92.9
MAE3D (DGCNN)	✓	1k	93.4 (+0.5)

respectively. These results offer compelling evidence that our method demonstrates efficacy with real-world data.

Few-shot learning. Following previous work [40], we fine-tune our pre-trained model via few-shot learning. We also use the “ K -way N -shot” setting, where K classes are randomly selected from the dataset, and then $(N + 20)$ samples are

TABLE III
CLASSIFICATION COMPARISON RESULTS OF OUR METHOD AND SUPERVISED METHODS ON MODELNET10.

Methods	# Points	Acc.
3D-GCN [35]	1k	93.9
SO-Net [32]	2k	94.1
KCNet [36]	1k	94.4
PointCNN [30]	1k	94.9
Point2Sequence [37]	1k	95.3
MAE3D	1k	95.5

TABLE IV
CLASSIFICATION COMPARISON RESULTS OF OUR METHOD AND SUPERVISED METHODS ON SCANOBJECTNN.

Methods	OBJ_ONLY	OBJ_BG	PB_T50_RS
3DmFV [38]	73.8	68.2	63.0
PointNet [1]	79.2	73.3	68.2
SpiderCNN [39]	79.5	77.1	73.7
PointNet++ [4]	84.3	82.3	77.9
PointCNN [30]	85.5	86.1	78.5
Point-BERT [13]	88.1	87.4	83.1
PointMask [16]	87.9	89.3	84.6
Point-MAE [15]	88.3	90.0	85.2
Point-M2AE [17]	88.8	91.2	86.4
DGCNN [2]	86.2	82.8	78.1
MAE3D (DGCNN)	88.4 (+2.2)	87.7 (+4.9)	86.2 (+8.1)

chosen for each class. Therefore, there are $K \times (N + 20)$ samples as the sub-dataset, with $K \times N$ samples as the training set and $K \times 20$ samples as the testing set. We adopt the dataset provided by PointBERT [13] to keep the same input as them. In our experiments, we also conduct 10 independent experiments and calculate the mean and the standard deviation over these 10 runs for 4 schemes: “5-way 10-shot”, “5-way 20-shot”, “10-way 10-shot”, and “10-way 20-shot”. The results are shown in Table V, from which we can see that our MAE3D soundly outperforms PointBERT, indicating that our method is able to learn more discriminative features in a limited dataset.

Linear classification evaluation. To verify that our pre-text task can effectively extract latent representations of point clouds, we use a linear classifier for 3D object classification, which follows the linear protocol on unsupervised learning. The pre-trained model is frozen and used to extract point cloud features, and only the linear classifier is trained.

Table VI shows the comparison results of our method and the SOTA methods. For a fair comparison, we have classified

TABLE V
COMPARISON RESULTS OF FEW-SHOT LEARNING ON MODELNET40. THE MEAN AND STANDARD DEVIATION OVER 10 INDEPENDENT EXPERIMENTS ARE SHOWN. THE DGCNN’S RESULTS ARE REPORTED IN POINTBERT.

Methods	5-way 10-shot	5-way 20-shot	10-way 10-shot	10-way 20-shot
DGCNN (rand) [13]	91.8 ± 3.7	93.4 ± 3.2	86.3 ± 6.2	90.9 ± 5.1
DGCNN (OcCo) [13]	91.9 ± 3.3	93.9 ± 3.1	86.4 ± 5.4	91.3 ± 4.6
Point-BERT [13]	94.6 ± 3.1	96.3 ± 2.7	91.0 ± 5.4	92.7 ± 5.1
Point-MAE [15]	96.3 ± 2.5	97.8 ± 1.8	92.6 ± 4.1	95.0 ± 3.0
MAE3D	95.2 ± 3.1	97.9 ± 1.6	91.1 ± 4.6	95.3 ± 3.1

TABLE VI
CLASSIFICATION COMPARISON RESULTS OF OUR METHOD AND UNSUPERVISED METHODS ON MODELNET40. SHAPENET55 AND MODELNET40 PRETRAINED CASES ARE PROVIDED.

Methods	Pre-trained dataset	Pre-text task	# Points	Acc.
FoldingNet [3]	ShapeNet55	reconstruction	2k	88.4
VIPGAN [41]	ShapeNet55	reconstruction	2k	90.2
LatentGAN [21]	ShapeNet55	reconstruction	2k	85.7
PointCapsNet [42]	ShapeNet55	reconstruction	2k	88.9
SSC (RSCNN) [34]	ShapeNet55	shape self-correction	2k	92.4
MAE3D (DGCNN)	ShapeNet55	reconstruction	2k	92.5
FoldingNet [3]	ModelNet40	reconstruction	2k	84.4
LatentGAN [21]	ModelNet40	reconstruction	2k	87.3
PointCapsNet [42]	ModelNet40	reconstruction	1k	87.5
MAP-VAE [20]	ModelNet40	reconstruction	2k	90.2
Multi-task [43]	ModelNet40	multiple	2k	89.1
PointHop [44]	ModelNet40	multiple	1k	89.1
GLR (RSCNN) [45]	ModelNet40	multiple	1k	92.2
MAE3D (DGCNN)	ModelNet40	reconstruction	1k	92.4

TABLE VII
COMPARISON OF 3D OBJECT CLASSIFICATION ACCURACY RESULTS WITH LIMITED TRAINING DATA (DIFFERENT RATIOS). THE RESULTS WITHOUT BEING REPORTED PREVIOUSLY ARE MARKED AS ‘-’.

Methods	1%	2%	5%	10%	20%
FoldingNet [3]	56.4	66.9	75.6	81.2	83.6
3DPatch [33]	65.2	-	-	84.4	-
MAE3D	61.7	69.2	80.8	84.7	88.3

the experimental results based on the pre-trained dataset. With the reconstruction as the pre-text task, our MAE3D significantly outperforms the other methods with pre-training on ShapeNet55, e.g., exceeding LatentGAN [21] by 6.8% and exceeding FoldingNet [3] by 4.1%.

We also perform an experiment for training on limited data using linear classifier, and the results can be seen in Table VII. Our MAE3D pre-trained model can achieve 88.3% with DGCNN [2] as backbone, even with only 20% data for training. Furthermore, in some extreme cases, i.e., using only 1% data, our method also achieves a good result of 61.7%, which exceeds FoldingNet [3] by 5.3%, but is lower than 65.2% of 3DPatch [33]. The reason is that MAE3D removes lots of point cloud patches (with 0.7 masking) during the pre-training, and only learns the features of a limited number of points. When processing the downstream classification task, a very small amount of data will greatly affect the data diversity and result in less performance improvement.

E. Shape Part Segmentation

We also conduct another downstream task, i.e., shape part segmentation, to further verify our method’s effectiveness. We use the mean Intersection-over-Union (mIoU) of instances as the evaluation metric. The results are reported in Table VIII which shows our MAE3D using DGCNN as the backbone improves over the original DGCNN by 0.4% in terms of mIoU of instances. Though our downstream network has no additional parameters compared to the backbone, i.e., no heavy-

TABLE VIII
SHAPE PART SEGMENTATION RESULTS OF OUR METHOD AND STATE-OF-THE-ART TECHNIQUES ON SHAPENET PART DATASET.

Methods	Instance mIOU	air.	bag	cap	car	chair	ear.	guit.	kni.	lam.	lap.	mot.	mug	pist.	rock.	ska.	tab.
Kd-Net [46]	82.3	80.1	74.6	74.3	70.3	88.6	73.5	90.2	87.2	81.0	84.9	87.4	86.7	78.1	51.8	69.9	80.3
PointNet [1]	83.7	83.4	78.7	82.5	74.9	89.6	73.0	91.5	85.9	80.8	95.3	65.2	93.0	81.2	57.9	72.8	80.6
SO-Net [32]	84.9	82.8	77.8	88.0	77.3	90.6	73.5	90.7	83.9	82.8	94.8	69.1	94.2	80.9	53.1	72.9	83.0
PointNet++ [4]	85.1	82.4	79.0	87.7	77.3	90.8	71.8	91.0	85.9	83.7	95.3	71.6	94.1	81.3	58.7	76.4	82.6
3D-GCN [35]	85.1	83.1	84.0	86.6	77.5	90.3	74.1	90.9	86.4	83.8	95.6	66.8	94.8	81.3	59.6	75.7	82.8
Point-BERT [13]	85.6	84.3	84.8	88.0	79.8	91.0	81.7	91.6	87.9	85.2	95.6	75.6	94.7	84.3	63.4	76.3	81.5
MaskPoint [16]	86.0	84.2	85.6	88.1	80.3	91.2	79.5	91.9	87.8	86.2	95.3	76.9	95.0	85.3	64.4	76.9	81.8
Point-MAE [15]	86.1	84.3	85.0	88.3	80.5	91.3	78.5	92.1	87.4	86.1	96.1	75.2	94.6	84.7	63.5	77.1	82.4
DGCNN [2]	85.2	84.0	83.4	86.7	77.8	90.6	74.7	91.2	87.5	82.8	95.7	66.3	94.9	81.1	63.5	74.5	82.6
MAE3D (DGCNN)	85.6 (+0.4)	83.7	81.7	85.3	78.5	90.8	80.1	91.4	89.1	84.6	95.5	66.7	94.8	81.9	58.5	74.6	82.7

weight Transformer blocks, we achieve comparable results to the recent Transformer-based methods like Point-BERT [13].

F. Ablation Studies

Masking. In this part, we show the results of two masking strategies with different masking ratios in Figure 4. It can be observed that using block masking can obtain better results in all cases, which has higher accuracy on the classification task. Besides, a high masking ratio, i.e., 0.7, works well on both block masking and random masking. It suggests that the challenge caused by a high masking ratio will benefit the network to capture the latent representations of the sample, which facilitates the classification results. We also calculated the Chamfer Distance for the reconstruction of these two strategies on the ShapeNet55 dataset [26] with the masking ratio of 0.7, and the results are shown in Table IX (cases A and B). It can be seen that block masking still performs better than random masking.

Loss. To verify the effectiveness of our proposed multi-task loss, we conduct an experiment on whether using center point loss. As shown in Table IX (cases C and D), the prediction of the center point for each patch serves a critical role, allowing the network to capture the geometric position relationship between each patch, which contributes to better results in the reconstruction of the entire point clouds, i.e., a smaller Chamfer Distance error.



Fig. 4. Comparison of different masking strategies and masking ratios on downstream classification task (with DGCNN as the backbone). The y-axis is ModelNet40 testing accuracy (%).

Patch size. We perform the ablation study on the number of points in each patch (i.e., patch size). A large patch size causes a large overlap of each patch in the split, which prevents the selected points from covering as many points as possible in the original point cloud. Fewer points per patch will affect the effectiveness of the patch feature extractor. In general, it is more difficult to learn features with fewer points as input. As shown in Table X, 64 points per patch is the best.

TABLE IX
COMPARISON RESULTS OF RANDOM/BLOCK MASKING AND THE DIFFERENT LOSS OPTIONS. THE CHAMFER DISTANCE IS CALCULATED ON SHAPENET55 FOR PRE-TRAINING WITH 0.7 MASKING RATIO. THE CLASSIFICATION ACCURACY IS CALCULATED ON MODELNET40.

Cases	Masking Strategies	Loss	CD ($\times 10^{-3}$)	Acc.
A	random	multi-task loss	3.260	93.2
B	block	multi-task loss	3.127	93.4
C	block	w/o center point	4.034	93.0
D	block	multi-task loss	3.127	93.4

TABLE X
COMPARISON RESULTS OF DIFFERENT PATCH SIZES. SHAPENET55 IS USED FOR PRE-TRAINING WITH BLOCK MASKING AND RATIO 0.7. MODELNET40 IS USED FOR FINE-TUNING WITH DGCNN AS BACKBONE.

#. patches	16	32	64	128
#. points per patch	128	64	32	16
Acc.(%)	92.9	93.4	93.2	93.1

Decoder design. We also conduct a study on our MAE3D decoder. Table XI studies the decoder depth (number of Transformer blocks) and decoder width (number of channels). The results indicate that 6 blocks and 1024 channels achieve the best performance.

Training with v.s. without the pre-trained model. Our pre-trained model can effectively improve the capability of the backbone. It is interesting to find that using our pre-trained parameters as initialization and then fine-tuning on downstream tasks can enable the model to capture the point cloud features at the beginning of the training process. As shown in Figure 5, the case with pre-training achieves better classification performance than training from scratch (i.e., original DGCNN [2]). The model can converge to the optimal solution more efficiently and accurately.

TABLE XI
COMPARISON RESULTS OF THE DECODER STRUCTURE. THE DECODER IS USED FOR THE COMPLETION TASK. SHAPENET55 IS USED FOR PRE-TRAINING, AND MODELNET40 IS USED FOR FINE-TUNING. THE CLASSIFICATION ACCURACY ON MODELNET40 IS USED HERE.

#. blocks	2	4	6	8	#. channels	512	1024	2048
Acc.(%)	93.3	92.9	93.4	92.9	Acc.(%)	92.7	93.4	92.8

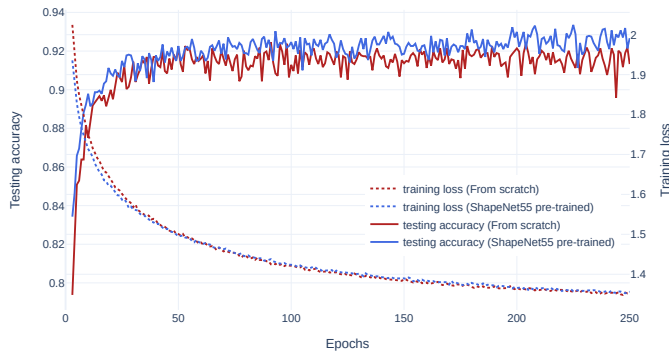


Fig. 5. Comparison with or without using pre-trained model for ModelNet40. The y-axes on the left/right are testing accuracy (%) and training loss, respectively.

TABLE XII

COMPARISON RESULTS OF WHETHER USING MAE3D TRANSFORMERS DURING PRE-TRAINING. SHAPENET55 IS USED FOR PRE-TRAINING WITH BLOCK MASKING AND RATIO 0.7.

Cases	Acc.
Without MAE3D Transformers	92.4
With MAE3D Transformers	93.4

Pre-training with v.s. without MAE3D Transformers.

We examine whether our MAE3D Transformers can predict the latent representations of the masked patches, i.e., a more complete and significant global feature of the point cloud can be obtained by MAE3D Transformers. We perform a comparison experiment to demonstrate this. As shown in Table XII, the network pre-training with MAE3D Transformers can achieve a better result, with a 1% improvement compared to the network without it.

Fine-tuning with v.s. without Transformer Encoder.

A significant contribution of our method is its ability to fine-tune downstream tasks using only the backbone network, without the complex transformer encoder, making our network more lightweight. As shown in Table XIII, Point-MAE [15] requires loading the transformer encoder, which contains 22.0M parameters (12 times more than ours of 1.8M), but we achieve improved results with a much more lightweight model.

For more comprehensive comparison, we reproduce Point-MAE by removing the transformer encoder but obtain subpar results. In contrast, our method can yield comparable results when loading the heavy transformer encoder. We hypothesize that the transformer encoder is focused on predicting the masked patches feature to reconstruct the point cloud in the pre-text task, while the backbone network primarily extracts the point cloud features. Without loading the transformer encoder, the learned point cloud features will not be excessively transformed by a complex network, resulting in a more intuitive point cloud feature representation.

Comparison with different feature extractors.

We perform an experiment comparing the backbone network used as the feature extractor in our model. For a fair comparison with Point-MAE [15], we employ PointNet [1] as the backbone network to extract features from the input points. Simultane-

TABLE XIII

COMPARISON RESULTS OF WHETHER USING TRANSFORMER ENCODER DURING FINE-TUNING.

Methods	Transformer Encoder	Params.	Acc.
Point-MAE [15]	✓	22.00 M	93.2
Point-MAE [15]	✗	0.67 M	92.5
MAE3D	✓	40.65 M	93.2
MAE3D	✗	1.80 M	93.4

TABLE XIV

COMPARISON WITH DIFFERENT FEATURE EXTRACTORS.

Methods	Feature extractor	Acc.
PointNet [1]	-	89.2
Point-MAE [15]	PointNet + Transformer	93.2
MAE3D	PointNet	90.6
DGCNN [2]	-	92.9
Point-MAE [15]	DGCNN + Transformer	93.1
MAE3D	DGCNN	93.4

ously, we reproduce Point-MAE by altering their encoder with DGCNN [2] and carrying out the complete pre-training and fine-tuning process. The results are displayed in Table XIV, which indicates that our method significantly outperforms Point-MAE by 0.3% when using DGCNN. We also achieve close results when PointNet is used as the backbone. It’s noteworthy that Point-MAE incorporates Transformer blocks in the encoder during fine-tuning, which aids the simple PointNet in extracting more comprehensive information.

G. Visualization

In Figure 6, we visualize the learned features on ModelNet40 [7] with t-SNE visualization. It can be seen that our MAE3D can separate different features relatively well even in the pre-training process, which indicates that our MAE3D Transformers can learn local features among point cloud patches without specific labels. It is interesting to observe that comparing with the original DGCNN [2] (i.e., training from scratch), our MAE3D could enable more separable features after fine-tuning, which implies that our pre-trained model can effectively facilitate the downstream task.

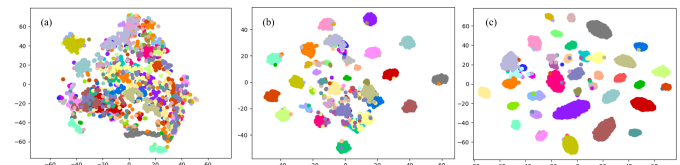


Fig. 6. T-SNE visualization of features learned by MAE3D and original DGCNN. (a) MAE3D pre-training, (b) original DGCNN, (c) MAE3D fine-tuning.

V. CONCLUSION

In this paper, we proposed MAE3D for point cloud self-supervised representation learning through the MPM pre-text task, which can learn the discriminative features of point cloud patches and the high-level contextual relationships between

patches. After pre-training, we load the pre-trained patch feature extractor and fine-tune it on the downstream task of 3D object classification, achieving state-of-the-art accuracy of 93.4% on ModelNet40 and 86.2% on ScanObjectNN (PB_T50_RS). This demonstrates the superiority of our proposed method over state-of-the-art methods.

ACKNOWLEDGMENTS

This work was supported by the National Key Research and Development Program of China (Grant Number 2022YFD1300200) and the Shaanxi Province Key Research and Development Program (Grant Number 2022QFY11-03).

REFERENCES

- [1] C. R. Qi, H. Su, K. Mo, and L. J. Guibas, "Pointnet: Deep learning on point sets for 3d classification and segmentation," in *Proceedings of the IEEE conference on computer vision and pattern recognition*, 2017, pp. 652–660. **1, 2, 4, 6, 7, 8, 9, 10**
- [2] Y. Wang, Y. Sun, Z. Liu, S. E. Sarma, M. M. Bronstein, and J. M. Solomon, "Dynamic graph cnn for learning on point clouds," *ACM Transactions on Graphics (TOG)*, 2019. **1, 2, 4, 6, 7, 8, 9, 10**
- [3] Y. Yang, C. Feng, Y. Shen, and D. Tian, "Foldingnet: Point cloud auto-encoder via deep grid deformation," 2018. **1, 3, 5, 6, 7, 8**
- [4] C. R. Qi, L. Yi, H. Su, and L. J. Guibas, "Pointnet++: Deep hierarchical feature learning on point sets in a metric space," 2017. **1, 2, 7, 8, 9**
- [5] M.-H. Guo, J.-X. Cai, Z.-N. Liu, T.-J. Mu, R. R. Martin, and S.-M. Hu, "Pct: Point cloud transformer," *Computational Visual Media*, vol. 7, no. 2, p. 187–199, Apr 2021. [Online]. Available: <http://dx.doi.org/10.1007/s41095-021-0229-5> **1, 2, 7**
- [6] W. Wu, Z. Qi, and L. Fuxin, "Pointconv: Deep convolutional networks on 3d point clouds," in *Proceedings of the IEEE/CVF Conference on Computer Vision and Pattern Recognition*, 2019, pp. 9621–9630. **1, 7**
- [7] Z. Wu, S. Song, A. Khosla, F. Yu, L. Zhang, X. Tang, and J. Xiao, "3d shapenets: A deep representation for volumetric shapes," in *Proceedings of the IEEE conference on computer vision and pattern recognition*, 2015, pp. 1912–1920. **1, 6, 10**
- [8] P.-S. Wang, Y. Liu, Y.-X. Guo, C.-Y. Sun, and X. Tong, "O-cnn," *ACM Transactions on Graphics*, vol. 36, no. 4, p. 1–11, Jul 2017. [Online]. Available: <http://dx.doi.org/10.1145/3072959.3073608> **1**
- [9] L. Jing and Y. Tian, "Self-supervised visual feature learning with deep neural networks: A survey," *IEEE Transactions on Pattern Analysis and Machine Intelligence*, vol. 43, no. 11, pp. 4037–4058, 2021. **1**
- [10] J. Devlin, M.-W. Chang, K. Lee, and K. Toutanova, "Bert: Pre-training of deep bidirectional transformers for language understanding," *arXiv preprint arXiv:1810.04805*, 2018. **1, 3**
- [11] H. Bao, L. Dong, and F. Wei, "Beit: Bert pre-training of image transformers," *arXiv preprint arXiv:2106.08254*, 2021. **1, 3**
- [12] K. He, X. Chen, S. Xie, Y. Li, P. Dollár, and R. Girshick, "Masked autoencoders are scalable vision learners," 2021. **1, 3, 4, 5**
- [13] X. Yu, L. Tang, Y. Rao, T. Huang, J. Zhou, and J. Lu, "Point-bert: Pre-training 3d point cloud transformers with masked point modeling," 2021. **1, 3, 6, 7, 8, 9**
- [14] K. He, H. Fan, Y. Wu, S. Xie, and R. Girshick, "Momentum contrast for unsupervised visual representation learning," in *Proceedings of the IEEE/CVF conference on computer vision and pattern recognition*, 2020, pp. 9729–9738. **1**
- [15] Y. Pang, W. Wang, F. E. Tay, W. Liu, Y. Tian, and L. Yuan, "Masked autoencoders for point cloud self-supervised learning," in *Computer Vision—ECCV 2022: 17th European Conference, Tel Aviv, Israel, October 23–27, 2022, Proceedings, Part II*. Springer, 2022, pp. 604–621. **1, 3, 5, 7, 8, 9, 10**
- [16] H. Liu, M. Cai, and Y. J. Lee, "Masked discrimination for self-supervised learning on point clouds," in *Computer Vision—ECCV 2022: 17th European Conference, Tel Aviv, Israel, October 23–27, 2022, Proceedings, Part II*. Springer, 2022, pp. 657–675. **1, 3, 8, 9**
- [17] R. Zhang, Z. Guo, P. Gao, R. Fang, B. Zhao, D. Wang, Y. Qiao, and H. Li, "Point-m2ae: multi-scale masked autoencoders for hierarchical point cloud pre-training," *arXiv preprint arXiv:2205.14401*, 2022. **1, 3, 7, 8**
- [18] A. Vaswani, N. Shazeer, N. Parmar, J. Uszkoreit, L. Jones, A. N. Gomez, Ł. Kaiser, and I. Polosukhin, "Attention is all you need," *Advances in neural information processing systems*, vol. 30, 2017. **3**
- [19] S. Qiu, S. Anwar, and N. Barnes, "Geometric back-projection network for point cloud classification," *IEEE Transactions on Multimedia*, 2021. **3**
- [20] Z. Han, X. Wang, Y.-S. Liu, and M. Zwicker, "Multi-angle point cloudvae: Unsupervised feature learning for 3d point clouds from multiple angles by joint self-reconstruction and half-to-half prediction," in *2019 IEEE/CVF International Conference on Computer Vision (ICCV)*. IEEE, 2019, pp. 10441–10450. **3, 8**
- [21] P. Achlioptas, O. Diamanti, I. Mitliagkas, and L. Guibas, "Learning representations and generative models for 3d point clouds," in *International conference on machine learning*. PMLR, 2018, pp. 40–49. **3, 8**
- [22] J. Jiang, X. Lu, W. Ouyang, and M. Wang, "Unsupervised representation learning for 3d point cloud data," *arXiv preprint arXiv:2110.06632*, 2021. **3**
- [23] A. Ramesh, M. Pavlov, G. Goh, S. Gray, C. Voss, A. Radford, M. Chen, and I. Sutskever, "Zero-shot text-to-image generation," 2021. **3**
- [24] A. Dosovitskiy, L. Beyer, A. Kolesnikov, D. Weissenborn, X. Zhai, T. Unterthiner, M. Dehghani, M. Minderer, G. Heigold, S. Gelly *et al.*, "An image is worth 16x16 words: Transformers for image recognition at scale," *arXiv preprint arXiv:2010.11929*, 2020. **3, 4, 5**
- [25] W. Yuan, T. Khot, D. Held, C. Mertz, and M. Hebert, "Pcn: Point completion network," in *2018 International Conference on 3D Vision (3DV)*. IEEE, 2018, pp. 728–737. **5, 6, 7**
- [26] A. X. Chang, T. Funkhouser, L. Guibas, P. Hanrahan, Q. Huang, Z. Li, S. Savarese, M. Savva, S. Song, H. Su *et al.*, "Shapenet: An information-rich 3d model repository," *arXiv preprint arXiv:1512.03012*, 2015. **6, 9**
- [27] M. A. Uy, Q.-H. Pham, B.-S. Hua, D. T. Nguyen, and S.-K. Yeung, "Revisiting point cloud classification: A new benchmark dataset and classification model on real-world data," in *International Conference on Computer Vision (ICCV)*, 2019. **6**
- [28] L. Yi, V. G. Kim, D. Ceylan, I.-C. Shen, M. Yan, H. Su, C. Lu, Q. Huang, A. Sheffer, and L. Guibas, "A scalable active framework for region annotation in 3d shape collections," *ACM Transactions on Graphics (ToG)*, vol. 35, no. 6, pp. 1–12, 2016. **6**
- [29] C. Chen, S. Qian, Q. Fang, and C. Xu, "Hapgn: Hierarchical attentive pooling graph network for point cloud segmentation," *IEEE Transactions on Multimedia*, 2020. **7**
- [30] Y. Li, R. Bu, M. Sun, W. Wu, X. Di, and B. Chen, "Pointcnn: Convolution on x-transformed points," *Advances in neural information processing systems*, vol. 31, 2018. **7, 8**
- [31] Y. Liu, B. Fan, S. Xiang, and C. Pan, "Relation-shape convolutional neural network for point cloud analysis," in *Proceedings of the IEEE/CVF Conference on Computer Vision and Pattern Recognition*, 2019, pp. 8895–8904. **7**
- [32] J. Li, B. M. Chen, and G. H. Lee, "So-net: Self-organizing network for point cloud analysis," in *Proceedings of the IEEE conference on computer vision and pattern recognition*, 2018, pp. 9397–9406. **7, 8, 9**
- [33] J. Sauder and B. Sievers, "Self-supervised deep learning on point clouds by reconstructing space," *Advances in Neural Information Processing Systems*, vol. 32, 2019. **7, 8**
- [34] Y. Chen, J. Liu, B. Ni, H. Wang, J. Yang, N. Liu, T. Li, and Q. Tian, "Shape self-correction for unsupervised point cloud understanding," in *Proceedings of the IEEE/CVF International Conference on Computer Vision*, 2021, pp. 8382–8391. **7, 8**
- [35] Z.-H. Lin, S.-Y. Huang, and Y.-C. F. Wang, "Convolution in the cloud: Learning deformable kernels in 3d graph convolution networks for point cloud analysis," in *Proceedings of the IEEE/CVF conference on computer vision and pattern recognition*, 2020, pp. 1800–1809. **8, 9**
- [36] Y. Shen, C. Feng, Y. Yang, and D. Tian, "Mining point cloud local structures by kernel correlation and graph pooling," in *Proceedings of the IEEE conference on computer vision and pattern recognition*, 2018, pp. 4548–4557. **8**
- [37] X. Liu, Z. Han, Y.-S. Liu, and M. Zwicker, "Point2sequence: Learning the shape representation of 3d point clouds with an attention-based sequence to sequence network," in *Proceedings of the AAAI conference on artificial intelligence*, vol. 33, no. 01, 2019, pp. 8778–8785. **8**
- [38] Y. Ben-Shabat, M. Lindenbaum, and A. Fischer, "3dmfv: Three-dimensional point cloud classification in real-time using convolutional neural networks," *IEEE Robotics and Automation Letters*, vol. 3, no. 4, pp. 3145–3152, 2018. **8**
- [39] Y. Xu, T. Fan, M. Xu, L. Zeng, and Y. Qiao, "Spidercnn: Deep learning on point sets with parameterized convolutional filters," in *Proceedings of the European Conference on Computer Vision (ECCV)*, 2018, pp. 87–102. **8**

- [40] C. Sharma and M. Kaul, "Self-supervised few-shot learning on point clouds," *Advances in Neural Information Processing Systems*, vol. 33, pp. 7212–7221, 2020. [7](#)
- [41] Z. Han, M. Shang, Y.-S. Liu, and M. Zwicker, "View inter-prediction gan: Unsupervised representation learning for 3d shapes by learning global shape memories to support local view predictions," *Proceedings of the AAAI Conference on Artificial Intelligence*, vol. 33, no. 01, 2019, pp. 8376–8384. [8](#)
- [42] Y. Zhao, T. Birdal, H. Deng, and F. Tombari, "3d point capsule networks," in *Proceedings of the IEEE/CVF Conference on Computer Vision and Pattern Recognition*, 2019, pp. 1009–1018. [8](#)
- [43] K. Hassani and M. Haley, "Unsupervised multi-task feature learning on point clouds," in *Proceedings of the IEEE/CVF International Conference on Computer Vision*, 2019, pp. 8160–8171. [8](#)
- [44] M. Zhang, H. You, P. Kadam, S. Liu, and C.-C. J. Kuo, "Pointhop: An explainable machine learning method for point cloud classification," *IEEE Transactions on Multimedia*, vol. 22, no. 7, pp. 1744–1755, 2020. [8](#)
- [45] Y. Rao, J. Lu, and J. Zhou, "Global-local bidirectional reasoning for unsupervised representation learning of 3d point clouds," in *Proceedings of the IEEE/CVF Conference on Computer Vision and Pattern Recognition*, 2020, pp. 5376–5385. [8](#)
- [46] R. Klokov and V. Lempitsky, "Escape from cells: Deep kd-networks for the recognition of 3d point cloud models," in *Proceedings of the IEEE International Conference on Computer Vision*, 2017, pp. 863–872. [9](#)

VI. BIOGRAPHY SECTION



Jincen Jiang is currently pursuing the Ph.D. degree with the National Centre for Computer Animation (NCCA), Bournemouth University, UK. He received the Master degree and the B.E. degree from the College of Information Engineering, Northwest A&F University, China, in 2023 and 2020 respectively. His research interests include computer graphics, geometric modeling, and 3D deep learning.



Xuequan Lu (Senior Member, IEEE) is a Senior Lecturer at the Department of Computer Science and IT, La Trobe University, Australia. He spent more than two years as a Research Fellow in Singapore. Prior to that, he earned his PhD at Zhejiang University (China) in June 2016. His research interests mainly fall into the category of visual computing, for example, geometry modeling, processing and analysis, animation/simulation, 2D data processing and analysis. More information can be found at <http://www.xuequanlu.com>.



Lizhi Zhao is currently working on the Ph.D. degree with the State Key Laboratory of Virtual Reality Technology and Systems, School of Computer Science and Engineering, Beihang University. He received his Master degree from the College of Information Engineering, Northwest A&F University, China. His research interests mainly include computer graphics, virtual reality, and computer vision.



Richard Dazeley received his Ph.D. in Computer Science from the University of Tasmania in 2007. He is widely recognised for his pioneering work in multiobjective reinforcement learning publishing several highly cited papers that helped established the field. He has also organised the multiple workshops in the field. He is an associate professor of Computer Science at Deakin University (Geelong) where he is the Deputy Leader of the Machine Intelligence Lab. He is also interested in prudence analysis, natural language processing, data analytics and security. He has received multiple awards including Australian Educator of the Year in 2016 from the Australian Computer Society.



Meili Wang (Member, IEEE) is a professor at College of Information Engineering, Northwest A&F University. She received her Ph.D. degree in computer animation in 2011 at the National Centre for Computer Animation, Bournemouth University. Her research interests include computer graphics, geometric modeling, image processing, visualization and virtual reality.